Learning Deep Non-Blind Image Deconvolution Without Ground Truths (Supplementary Materials)

Yuhui Quan[1], Zhuojie Chen[1], Huan Zheng[2], and Hui Ji[2]

[1] School of Computer Science and Engineering, South China University of Technology, Guangzhou 510006, China
[2] Department of Mathematics, National University of Singapore, 119076, Singapore
csyhquan@scut.edu.cn, zhuojie.chen.cs@foxmail.com, huan_zheng@u.nus.edu, matjh@nus.edu.sg

1 Proof of Proposition 1

Proof. Without loss of generality, we prove for the 1D case where $\boldsymbol{Y}, \boldsymbol{X}, \boldsymbol{K}^*, \boldsymbol{N}, \boldsymbol{U}$ are vectors. The extension to 2D case is straightforward. Denote $\widehat{\boldsymbol{N}} = \boldsymbol{N} + \boldsymbol{U}$ and $\widetilde{\boldsymbol{N}} = \boldsymbol{N} - \boldsymbol{U}$, *i.e.*,

$$\begin{pmatrix} \widehat{\boldsymbol{N}} \\ \widetilde{\boldsymbol{N}} \end{pmatrix} = \begin{pmatrix} \boldsymbol{I} & \boldsymbol{I} \\ \boldsymbol{I} & -\boldsymbol{I} \end{pmatrix} \begin{pmatrix} \boldsymbol{N} \\ \boldsymbol{U} \end{pmatrix}. \tag{1}$$

Recall that $\boldsymbol{N}$ and $\boldsymbol{U}$ are i.i.d. Gaussian noise with zero mean and variance $\boldsymbol{\Sigma}$. It yields that

$$\begin{pmatrix} \boldsymbol{N} \\ \boldsymbol{U} \end{pmatrix} \sim \mathcal{N}\left(\begin{pmatrix} \boldsymbol{0} \\ \boldsymbol{0} \end{pmatrix}, \begin{pmatrix} \boldsymbol{\Sigma} & \boldsymbol{0} \\ \boldsymbol{0} & \boldsymbol{\Sigma} \end{pmatrix} \right). \tag{2}$$

Thus the joint distribution of $\widehat{\boldsymbol{N}}$ and $\widetilde{\boldsymbol{N}}$ is still Gaussian:

$$\begin{pmatrix} \widehat{\boldsymbol{N}} \\ \widetilde{\boldsymbol{N}} \end{pmatrix} \sim \mathcal{N}\left(\begin{pmatrix} \boldsymbol{0} \\ \boldsymbol{0} \end{pmatrix}, \boldsymbol{\Sigma}' \right), \tag{3}$$

where

$$\boldsymbol{\Sigma}' = \begin{pmatrix} \boldsymbol{I} & \boldsymbol{I} \\ \boldsymbol{I} & -\boldsymbol{I} \end{pmatrix} \begin{pmatrix} \boldsymbol{\Sigma} & \boldsymbol{0} \\ \boldsymbol{0} & \boldsymbol{\Sigma} \end{pmatrix} \begin{pmatrix} \boldsymbol{I} & \boldsymbol{I} \\ \boldsymbol{I} & -\boldsymbol{I} \end{pmatrix} = \begin{pmatrix} 2\boldsymbol{\Sigma} & \boldsymbol{0} \\ \boldsymbol{0} & 2\boldsymbol{\Sigma} \end{pmatrix}. \tag{4}$$

Hence we have that $\widehat{\boldsymbol{N}}$ and $\widetilde{\boldsymbol{N}}$ are independent, which leads to

$$\begin{aligned}
&\mathbb{E}_{\boldsymbol{N},\boldsymbol{U}} (\boldsymbol{N} - \boldsymbol{U})^\top (\boldsymbol{K}^* \otimes (\mathcal{F}(\boldsymbol{K}^* \otimes \boldsymbol{X} + \boldsymbol{N} + \boldsymbol{U}) - \boldsymbol{X})) \\
=&\mathbb{E}_{\widehat{\boldsymbol{N}},\widetilde{\boldsymbol{N}}} \widetilde{\boldsymbol{N}}^\top (\boldsymbol{K}^* \otimes (\mathcal{F}(\boldsymbol{K}^* \otimes \boldsymbol{X} + \widehat{\boldsymbol{N}}) - \boldsymbol{X})) \\
=&\mathbb{E}_{\widehat{\boldsymbol{N}}} \mathbb{E}_{\widetilde{\boldsymbol{N}}} \widetilde{\boldsymbol{N}}^\top (\boldsymbol{K}^* \otimes (\mathcal{F}(\boldsymbol{K}^* \otimes \boldsymbol{X} + \widehat{\boldsymbol{N}}) - \boldsymbol{X})) \\
=&\big(\mathbb{E}_{\widetilde{\boldsymbol{N}}} \widetilde{\boldsymbol{N}}\big)^\top \mathbb{E}_{\widehat{\boldsymbol{N}}} (\boldsymbol{K}^* \otimes (\mathcal{F}(\boldsymbol{K}^* \otimes \boldsymbol{X} + \widehat{\boldsymbol{N}}) - \boldsymbol{X})) \\
=&\boldsymbol{0}^\top \mathbb{E}_{\widehat{\boldsymbol{N}}} (\boldsymbol{K}^* \otimes (\mathcal{F}(\boldsymbol{K}^* \otimes \boldsymbol{X} + \widehat{\boldsymbol{N}}) - \boldsymbol{X})) = 0.
\end{aligned}$$

Then we can rewrite the loss $\mathcal{L}^{\mathrm{r}}$ as follows:

$$\begin{aligned}
&\mathbb{E}_{\boldsymbol{N},\boldsymbol{U}}\|\boldsymbol{K}^{*}\otimes\mathcal{F}(\boldsymbol{Y}+\boldsymbol{U})-(\boldsymbol{Y}-\boldsymbol{U})\|_{\mathrm{F}}^{2}\\
=&\mathbb{E}_{\boldsymbol{N},\boldsymbol{U}}\|\boldsymbol{K}^{*}\otimes(\mathcal{F}(\boldsymbol{K}^{*}\otimes\boldsymbol{X}+\boldsymbol{N}+\boldsymbol{U})-\boldsymbol{X})-(\boldsymbol{N}-\boldsymbol{U})\|_{\mathrm{F}}^{2}\\
=&\mathbb{E}_{\boldsymbol{N},\boldsymbol{U}}\Big\{\|\boldsymbol{K}^{*}\otimes(\mathcal{F}(\boldsymbol{K}^{*}\otimes\boldsymbol{X}+\boldsymbol{N}+\boldsymbol{U})-\boldsymbol{X})\|_{\mathrm{F}}^{2}\\
&-2(\boldsymbol{N}-\boldsymbol{U})^{\top}(\boldsymbol{K}^{*}\otimes(\mathcal{F}(\boldsymbol{K}^{*}\otimes\boldsymbol{X}+\boldsymbol{N}+\boldsymbol{U})-\boldsymbol{X}))\\
&+(\boldsymbol{N}-\boldsymbol{U})^{\top}(\boldsymbol{N}-\boldsymbol{U})\Big\}\\
=&\mathbb{E}_{\boldsymbol{N},\boldsymbol{U}}\|\boldsymbol{K}^{*}\otimes(\mathcal{F}(\boldsymbol{K}^{*}\otimes\boldsymbol{X}+\boldsymbol{N}+\boldsymbol{U})-\boldsymbol{X})\|_{\mathrm{F}}^{2}+2\mathrm{Trace}(\boldsymbol{\Sigma}).
\end{aligned}$$

The proof is done by noting $\mathbb{E}_{\boldsymbol{N},\boldsymbol{U}}(\boldsymbol{N}-\boldsymbol{U})^{\top}(\boldsymbol{N}-\boldsymbol{U})=2\mathrm{Trace}(\boldsymbol{\Sigma})$ is a constant. $\square$

2 Performance Gain versus Ensemble Size in Inference

Fig. 2 shows how the performance of UNID scales up with the increase of ensemble size (*i.e.* the number of inferences) in the ensemble inference on Levin *et al.*'s and Lai *et al.*'s datasets. It can be seen that with more inferences used for averaging, the overall performance increases and then becomes stable with a sufficient number of inferences for averaging.

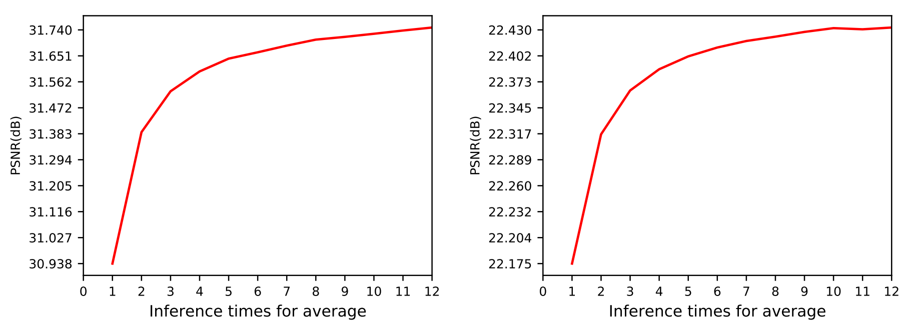

(a) (b)

Fig. 1. PSNR versus ensemble size in ensemble inference on (a) Levin *et al.*'s dataset with kernels estimated by [5] and (b) Lai *et al.*'s dataset with kernels estimated by [7]

3 Visual Comparison on More Images

See Fig. 2-3 for the results on motion deblurring with erroneous kernels, Fig. 4-6 for the results on motion deblurring with accurate kernels, and Fig. 7-10 for the deblurring results on some real samples. The visual quality achieved by UNID is quite competitive to that by the supervised methods.

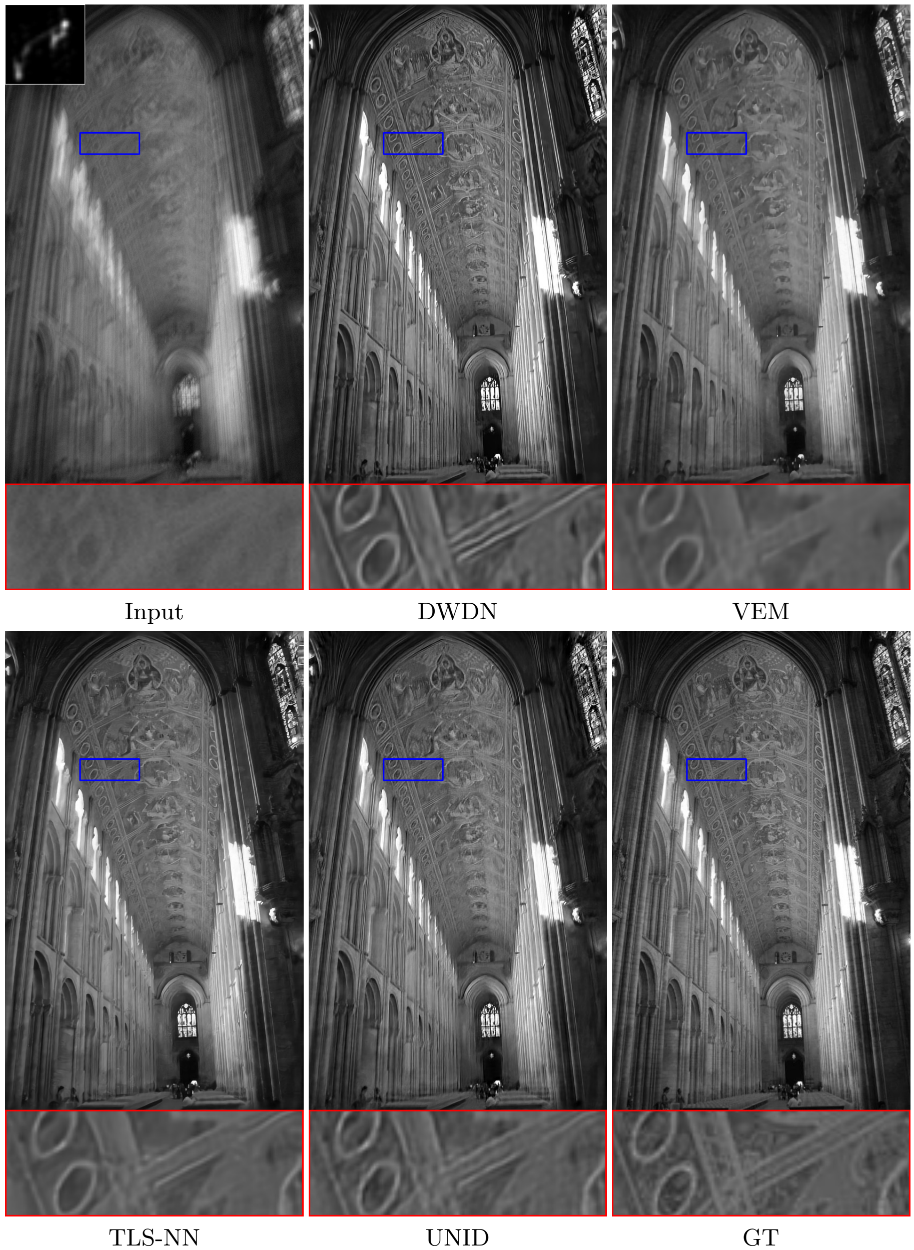

Fig. 2. NBID results on an image from Sun *et al.*'s dataset [6] with WG noise of $\sigma = 2.55$ and erroneous blur kernel of size 27×27 estimated by [7]

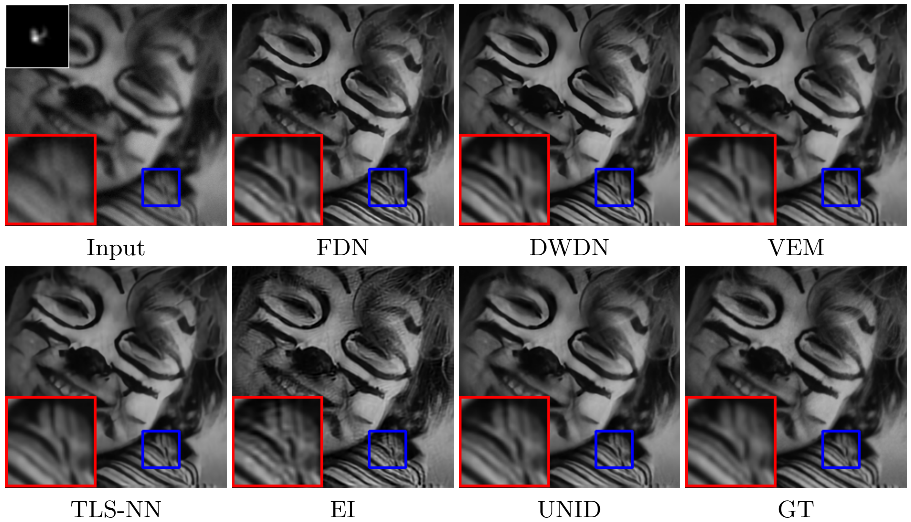

Fig. 3. NBID results on an image from Levin *et al.*'s dataset [2] with WG noise of $\sigma = 2.55$ and erroneous blur kernel of size 13×13 estimated by [6]

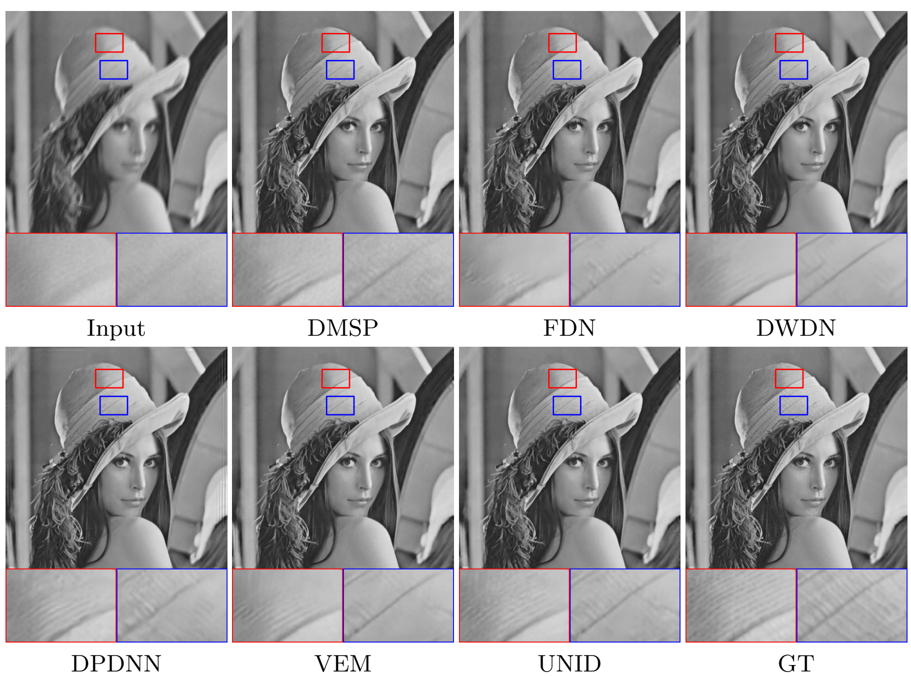

Fig. 4. NBID results on an image from Set12 [3] with WG noise of $\sigma = 2.55$ and an accurate blur kernel of size 19×19

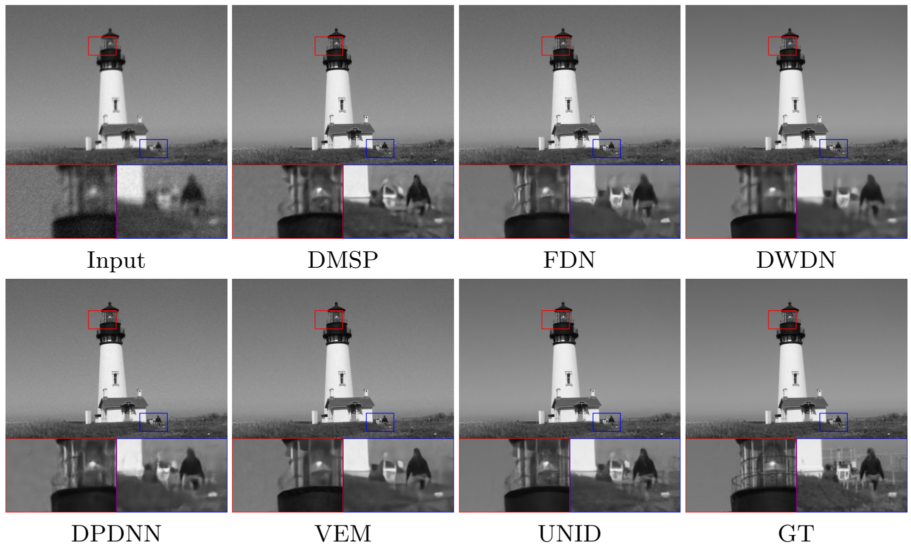

Fig. 5. NBID results for Sun *et al.*'s dataset [6] with WG noise of $\sigma = 7.65$ and an accurate blur kernel of size 15×15

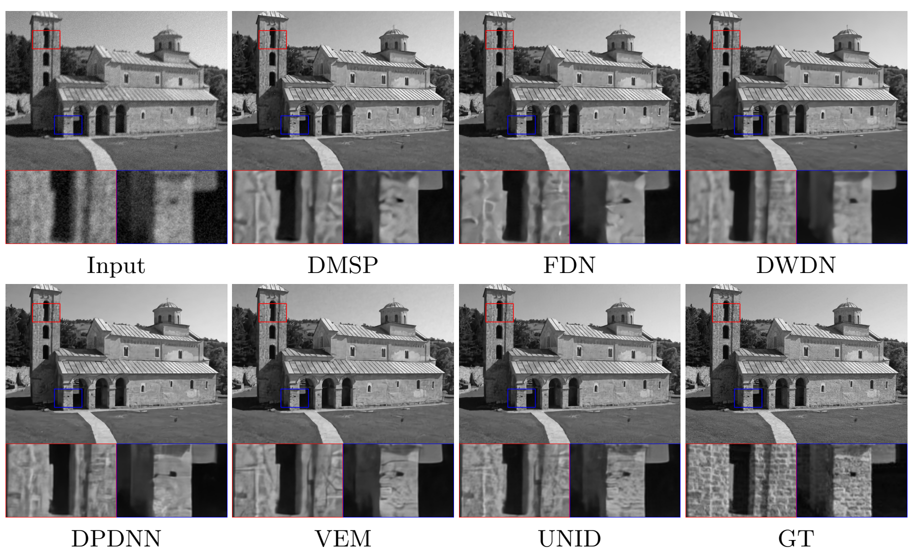

Fig. 6. NBID results for Sun *et al.*'s dataset [6] with WG noise of $\sigma = 12.75$ and an accurate blur kernel of size 15×15

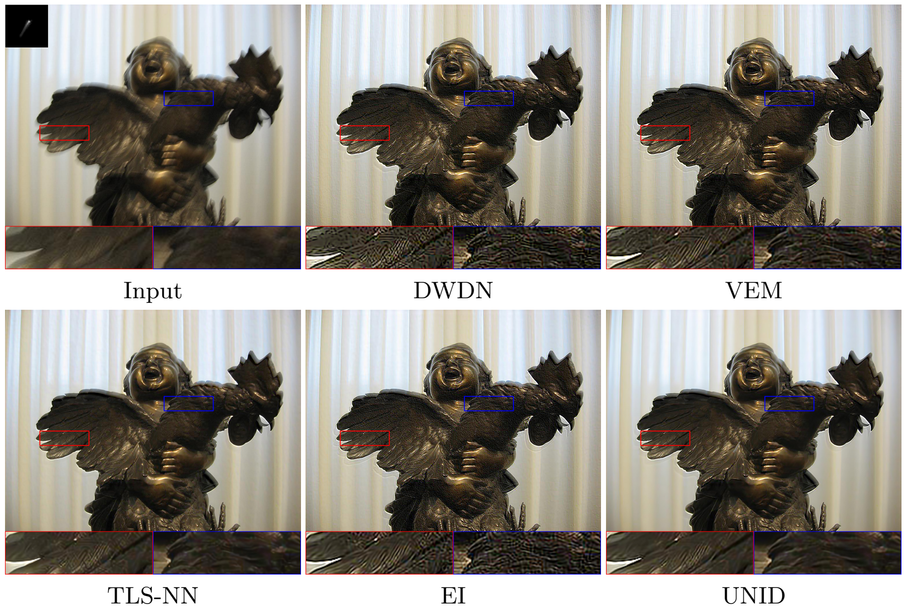

Fig. 7. NBID results on an image "boy_statue" from the real dataset in Lai *et al.*'s [1] with an erroneous blur kernel estimated by [4]

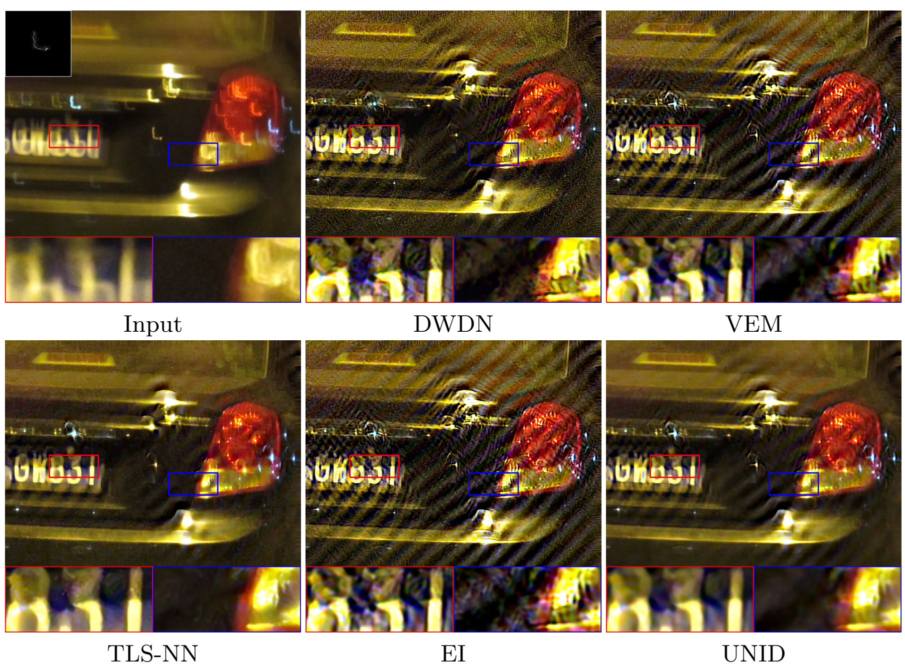

Fig. 8. NBID results on an image "car5" from the real dataset in Lai *et al.*'s [1] with an erroneous blur kernel estimated by [5]

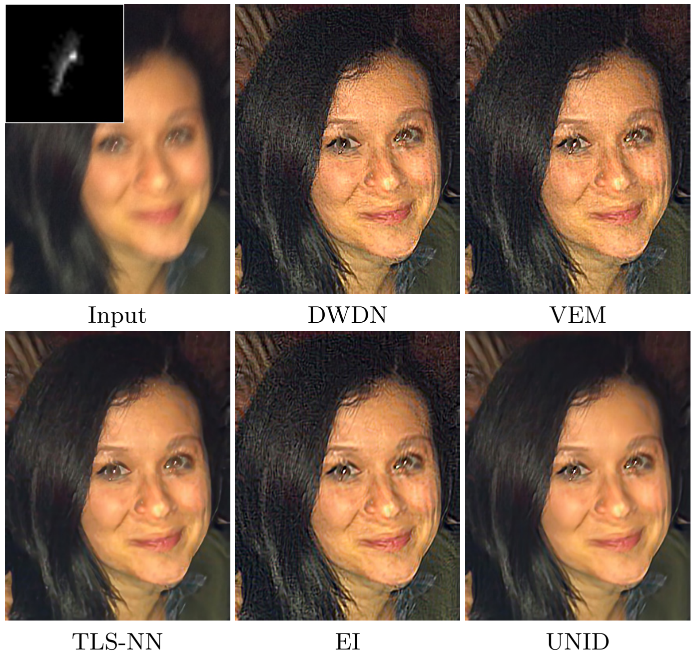

Fig. 9. NBID results on a patch of "face" from the real dataset in Lai *et al.*'s [1] with an erroneous blur kernel estimated by [5]

Fig. 10. NBID results on an image "cross_stitch" from the real dataset in Lai *et al.*'s [1] with an erroneous blur kernel estimated by [7]

References

1. Lai, W.S., Huang, J.B., Hu, Z., Ahuja, N., Yang, M.H.: A comparative study for single image blind deblurring. In: Proceedings of the IEEE Conference on Computer Vision and Pattern Recognition. pp. 1701–1709 (2016)
2. Levin, A., Weiss, Y., Durand, F., Freeman, W.T.: Efficient marginal likelihood optimization in blind deconvolution. In: Proceedings of the IEEE Conference on Computer Vision and Pattern Recognition. pp. 2657–2664. IEEE (2011)
3. Nan, Y., Quan, Y., Ji, H.: Variational-em-based deep learning for noise-blind image deblurring. In: Proceedings of the IEEE/CVF Conference on Computer Vision and Pattern Recognition. pp. 3626–3635 (2020)
4. Pan, J., Hu, Z., Su, Z., Yang, M.H.: Deblurring text images via l0-regularized intensity and gradient prior. In: Proceedings of the IEEE Conference on Computer Vision and Pattern Recognition. pp. 2901–2908 (2014)
5. Pan, J., Sun, D., Pfister, H., Yang, M.H.: Blind image deblurring using dark channel prior. In: Proceedings of the IEEE Conference on Computer Vision and Pattern Recognition. pp. 1628–1636 (2016)
6. Sun, L., Cho, S., Wang, J., Hays, J.: Edge-based blur kernel estimation using patch priors. In: Proceedings of the IEEE International Conference on Computational Photography. pp. 1–8. IEEE (2013)
7. Xu, L., Jia, J.: Two-phase kernel estimation for robust motion deblurring. In: Proceedings of the European Conference on Computer Vision. pp. 157–170. Springer (2010)